

PARAMETRIC INVESTIGATION TO OPTIMIZE THE
DYNAMIC RANGE OF MR DAMPER FOR VIBRATION
CONTROL

BY

MUHAMMAD KHUSYAIE BIN MOHD RAZALI

A thesis submitted in fulfillment of the requirement for the
degree of Master of Science (Mechatronics Engineering)

Kulliyyah of Engineering
International Islamic University Malaysia

OCTOBER 2020

ABSTRACT

This research sought to identify the solution of shock absorption for vibration control (in this case, to reduce the effect of the heel strike of the transtibial amputee in walking). This research proposes a device which is a damper-based shock absorber installing on a prosthetic limb that will be used by the transtibial amputee. The prosthetic leg adopts a semi-active damper to capture the advantages of passive damper along with to perform as good as an active damper. Magnetorheological (MR) damper, which utilizes the benefits of MR fluids, is one of the most promising semi-active devices in mitigating the vibration. MR fluids is a smart material because of the ability to control the rheological properties by tuning the external magnetic field strength. Moreover, mechanical simplicity, fast response, and low power consumption have attracted more interest on this damper. However, the challenging aspect of utilizing this device is to understand their performance under varied input parameters. Understanding the behavior of the MR damper is the critical feature to use this damper fully. A well-known mathematical model, the Phenomenological (Modified Bouc-Wen) model, is used to model the MR damper behavior. To use this model, a relationship between the damper parameters, including force, displacement, velocity, current, and frequency, should be available. An experimental study of MR damper is done by the researcher to acquire those relationships. A comprehensive optimization methodology to estimate the parameters of the Modified Bouc-Wen model is necessary. The researcher compares two optimization algorithm, which is Particle Swarm Optimization (PSO) and Genetic Algorithm (GA) to estimate the parameters. From the comparison, PSO, inspired by the behavior of bees swarming for the optimization methods, has higher accuracy, which is 95.92% compared to GA, which is 94.71%. The precision of the optimization of the Modified Bouc-Wen parameters is from 92.3% to 96.5%. Each parameter fits the function of input current and frequency using the polynomial equation (maximum 3rd polynomial order). The precision of the fitting is from 87% to 98.4%. Robust Controller is developed to control the MR damper for transtibial prosthetic limbs. In this research, prosthetic limb applications adapt H_∞ robust controller and inverse MR damper model. The result of the controller design compared to the targeted behavior is up to 92.51% accuracy. The simulation's performance is presumed to be acceptable since it almost followed the pattern of the targeted design.

ملخص البحث

هذا البحث سعى إلى تحديد حل امتصاص الصدمات للتحكم في الاهتزاز (في هذه الحالة، لتقليل تأثير ضربة الكعب للبتير العضلي أثناء المشي). يقترح هذا البحث على جهاز قائم على المخمد لامتصاص الصدمات والتي يتم تركيبها على طرف صناعي يتم استخدامه بواسطة العضو المبتور. تعتمد الساق الصناعية على مخمد نصف نشط لالتقاط المزايا المخمد سلبي كداء جيدة مثل المخمد النشط. MR) Magnetorheological (التي تستخدم فوائد سوائل الرنين المغناطيسي، وتعتبر هي أحد أكثر الأجهزة الواعدة شبه النشطة في تخفيف الاهتزاز. موائع MR مادة ذكية لأن قدرتها في التحكم على خصائص الروماتيزم بضبط قوة المغناطيسي الخارجي. بالإضافة إلى ذلك، البساطة الميكانيكية والاستجابة السريعة وانخفاض استهلاك للطاقة عمل جذب مهم لهذا المخمد. ومع ذلك، فإن أشد جوانب التحدي في استخدام هذا الجهاز هو فهم أدائها عند تغيير بعض المدخلات. إن فهم سلوك MR المخمد هي الميزة الأساسية لاستخدام هذا المخمد بالكامل. و المعرفة الكاملة بالنموذج الرياضي معروف وهو نموذج (Modified-Bouc-Wen) يُستخدم هذا النموذج لمعالجة سلوك المخمد MR. لاستخدام هذا النموذج، يجب أن تتوفر علاقة بين معاملات المخمد، بما في ذلك القوة والازاحة والسرعة والتيار والتردد. يتم إجراء دراسة تجريبية لمخمد MR من الباحث لاكتساب تلك العلاقات. ومنهج التحسين الشامل أمر ضروري. في تقدير معاملات نموذج Bouc-Wen المعدل. ويقارن الباحث بين خوارزميتين المحسنتين Particle Swarm Optimization (PSO) وخوارزمية الجينية (GA) لتقدير المعاملات. ومن خلال المقارنة، PSO، مستوحاة من سلوك احتشاد النحل لأسلوب التحسين، لذلك لديه الدقة أعلى وهي 95.92% مقارنة بGA وهي 94.71%. ودقة التحسين من Bouc-Wen معدل المعلمة وهي من 92.3% إلى 96.5%. ويناسب كل معامل وظيفة إدخال التيار والتردد باستخدام معادلة متعددة الحدود (أكثر معادلة متعددة الحدود الثالث). ودقة الاحكام من 87% إلى 98.4%. تحكم قوى تم تطويره للتحكم في المخمد MR لاجل الأطراف الصناعية. في هذا البحث، التطبيقات الأطراف الصناعية يكيف H_{∞} وعكس نموذج المخمد MR. ونتيجة تصميم وحدة التحكم مقارنة بالسلوك المستهدف تصل إلى 92.51%. ويفترض أن أداء المحاكاة مقبول لأنها تتبع تقريباً بنمط التصميم المستهدف.

APPROVAL PAGE

I certify that I have supervised and read this study and that in my opinion, it conforms to acceptable standards of scholarly presentation and is fully adequate, in scope and quality, as a thesis for the degree of Master of Science (Mechatronics Engineering).

.....
Asan Gani Abdul Muthalif
Supervisor

.....
Syamsul Bahrin Bin Abdul
Hamid
Co-Supervisor

.....
Nor Hidayati Diyana Binti Nordin
Co-Supervisor

I certify that I have read this study and that in my opinion it conforms to acceptable standards of scholarly presentation and is fully adequate, in scope and quality, as a thesis for the degree of Master of Science (Mechatronics Engineering).

.....
Muhammad Mahbubur Rashid
Internal Examiner

.....
Rahizar Ramli
External Examiner

This thesis was submitted to the Department of Mechatronics Engineering and is accepted as a fulfillment of the requirement for the degree of Master of Science (Mechatronics Engineering).

.....
Syamsul Bahrin Bin Abdul
Hamid
Head, Department of
Mechatronics Engineering

This thesis was submitted to the Kulliyah of Engineering and is accepted as a fulfillment of the requirement for the degree of Master of Science (Mechatronics Engineering).

.....
Sany Izan Ihsan
Dean, Kulliyah of Engineering

DECLARATION

I hereby declare that this thesis is the result of my own investigations, except where otherwise stated. I also declare that it has not been previously or concurrently submitted as a whole for any other degrees at IIUM or other institutions.

Muhammad Khusyaie Bin Mohd Razali

Signature

Date

INTERNATIONAL ISLAMIC UNIVERSITY MALAYSIA

**DECLARATION OF COPYRIGHT AND AFFIRMATION OF
FAIR USE OF UNPUBLISHED RESEARCH**

**PARAMETRIC INVESTIGATION TO OPTIMIZE THE
DYNAMIC RANGE OF MR DAMPER FOR VIBRATION**

I declare that the copyright holders of this thesis are jointly owned by the student and IIUM.

Copyright © 2020 Muhammad Khusyaie Bin Mohd Razali and International Islamic University Malaysia. All rights reserved.

No part of this unpublished research may be reproduced, stored in a retrieval system, or transmitted, in any form or by any means, electronic, mechanical, photocopying, recording or otherwise without prior written permission of the copyright holder except as provided below

1. Any material contained in or derived from this unpublished research may be used by others in their writing with due acknowledgement.
2. IIUM or its library will have the right to make and transmit copies (print or electronic) for institutional and academic purposes.
3. The IIUM library will have the right to make, store in a retrieved system and supply copies of this unpublished research if requested by other universities and research libraries.

By signing this form, I acknowledged that I have read and understand the IIUM Intellectual Property Right and Commercialization policy.

Affirmed by Muhammad Khusyaie Bin Mohd Razali

.....
Signature

.....
Date

ACKNOWLEDGEMENTS

First of all, Alhamdulillah and all praise to “ALLAH” S.W.T, the Most Beneficial and Most Merciful, to give me the ability and knowledge to accomplish my research work successfully.

I wish to express my appreciation and thanks to my supervisor Dr. Asan Gani bin Abdul Muthalif his dedicated guidance, suggestion, motivation and valuable support which have directed me the way to develop my research skills and knowledge as well.

I also like to thank my co-supervisor Dr. Syamsul Bahrin Abdul Hamid and Dr. Nor Hidayati Diyana Binti Nordin for their endless encouragement and support to my research work.

I wish to express my appreciation and thanks to those who provided their time, effort and support for this project. To the members Smart Structures, Systems and Control Research Laboratory (S³CRL), thank you for sticking with me.

Finally, it is my utmost pleasure to dedicate this work to my dear parents and my family, especially my wife, Afifah Abdullah who granted me the gift of their unwavering belief in my ability to accomplish this goal: thank you for your support and patience.

TABLE OF CONTENTS

Abstract	ii
ملخص البحث.....	iii
Approval Page.....	iv
Declaration	v
Acknowledgements	vii
Table of Contents	viii
List of Tables	x
List of Figures	xi
List of Symbols	xvi
List of Abbreviations	xvii
CHAPTER ONE: INTRODUCTION	1
1.1 Background of The Study	1
1.2 Problem Statement.....	5
1.3 Research Objectives.....	6
1.4 Research Methodology	7
1.5 Organization of the Thesis.....	9
CHAPTER TWO: LITERATURE REVIEW	10
2.1 Introduction.....	10
2.2 Magnetorheological (MR) Fluids	10
2.2.1 MR Fluid Applications.....	12
2.2.2 MR Fluid Compositions.....	13
2.2.3 MR Fluid Operational Mode.....	15
2.2.4 MR Fluid Analytical Models	16
2.2.5 MR Fluid and Temperature Effect	18
2.3 Magnetorheological Fluid (MR) Damper Models	22
2.3.1 Bingham Model.....	24
2.3.2 Bouc-Wen Model.....	25
2.3.3 Phenomenological or Modified Bouc-Wen Model.....	26
2.3.4 Hyperbolic Tangent Function Model.....	27
2.4 Optimization Algorithm	28
2.4.1 Particle Swarm Optimization (PSO).....	30
2.5 Control Algorithm for Semi-active Devices.....	33
2.5.1 H-Infinity (H_∞) Robust Controller	36
2.5.2 Inverse MR Damper Model	38
2.6 Chapter Summary	39
CHAPTER THREE: EXPERIMENT ON MR DAMPER CHARACTERISTICS.....	40
3.1 Introduction.....	40
3.2 Magnetorheological (MR) Damper	40
3.3 Experimental Setup.....	42
3.4 Experimental Results	44
3.4.1 Force Response at Varying Input Current.....	44

3.4.2 Force Response at Varying Excitation Frequency	52
3.4.3 Energy Dissipation	58
3.5 Chapter Summary	60
CHAPTER FOUR: PARAMETRIC MODEL OPTIMIZATION	61
4.1 Introduction.....	61
4.2 Optimization Methodology.....	61
4.2.1 Objective Function	61
4.2.2 Parametric Model	62
4.2.3 Optimization Algorithm.....	63
4.2.4 Curve Fitting	63
4.2.5 Methodology	63
4.3 Optimization Result	65
4.4 Chapter Summary	76
CHAPTER FIVE: ROBUST CONTROLLER DESIGN.....	77
5.1 Introduction.....	77
5.2 Transtibial Prosthetic Limbs Model	77
5.3 Control Algorithm	80
5.4 Simulation Study	87
5.4.1 H-infinity Controller Simulation.....	87
5.4.2 Inverse Modified Bouc Wen Model Simulation	90
5.4.3 Prosthetic Limb Simulation for Different Body Mass and Walking Speed.....	91
CHAPTER SIX: CONCLUSION	101
6.1 Conclusions	101
6.2 Contribution of Research	102
6.3 Limitation and Recommendations	102
REFERENCES.....	104
APPENDIX A	120
APPENDIX B	121

LIST OF TABLES

Table 3.1	Typical properties of MR damper RD-8040-1 (LORD Corporation, 2009b).	41
Table 3.2	Electrical properties of MR damper RD-8040-1 (LORD Corporation, 2009b).	41
Table 4.1	Normalized fitting error for each parameters of Modified Bouc-Wen model.	69
Table 4.2	The optimization error and the accuracy of the predicted model.	74
Table 5.1	The list of design parameters.	80

LIST OF FIGURES

Figure 1.1	Passive transtibial prosthetic limbs (ESAR) (left side) and active transtibial prosthetic limbs (right side) (retrieved from “Feet and Ankles”, 2018).	2
Figure 1.2	Positions of legs during single gait cycle (blue) (Pirker & Katzenschlager, 2016).	3
Figure 1.3	Plot of vertical ground reaction force (N) against time (ms) (Whittle, 2007).	4
Figure 1.4	The complete flow chart of the research methodology.	8
Figure 2.1	The orientation of magnetic particles; (a) without and (b) with a magnetic field (retrieved from “Magnetorheological fluids and devices”, (2014)).	11
Figure 2.2	Typical behavior of MR fluid in presence of magnetic field strength (H) in (a) Pre-yield and post-yield region using stress-strain curve and (b) post-yield region using stress-rate curve (D. H. Wang & Liao, 2011).	12
Figure 2.3	Operational mode of MR fluid as: (a) valve mode, (b) shear mode and (c) squeeze mode (Vicente, López, Reyes, Gutiérrez, & Alvarez, 2011).	16
Figure 2.4	Bingham plastic model and Herschel-Bulkley model of MR fluid (Nguyen & Choi, 2012).	17
Figure 2.5	Biviscous model of MR fluid (D. H. Wang & Liao, 2011).	18
Figure 2.6	The magnetization of iron particles with varying temperature for an external magnetic field of 1, 2 and 3 A/m (Coey, 2009).	20
Figure 2.7	Pressure versus temperature plots of Silicone oil (Kiciński, 2015).	21
Figure 2.8	General configuration of MR damper (Truong & Ahn, 2012).	23
Figure 2.9	The schematic diagram of Bingham model (Marinca et al., 2015).	25
Figure 2.10	Schematic diagram of Bouc-Wen model (Talatahari, Kaveh, & Rahbari, 2012).	26

Figure 2.11	Schematic diagram of Phenomenological or Modified Bouc-Wen model (Spencer et al., 1997).	27
Figure 2.12	Schematic diagram of Hyperbolic Tangent Function model (Kwok et al., 2006).	28
Figure 2.13	The flowchart of the PSO algorithm (Kalatehjari, Rashid, Ali, & Hajihassani, 2014).	32
Figure 2.14	The standard configuration of H_{∞} controller (V. P. Singh, Mohanty, Kishor, & Ray, 2013).	37
Figure 2.15	The block diagram of semi-active control for MR damper (Fallah et al., 2012).	38
Figure 3.1	The photograph of Magnetorheological Fluid (MR) damper RD-8040-1.	40
Figure 3.2	The schematic drawing of MR damper RD-8040-1 (Note that the dimension is in mm)(LORD Corporation, 2009a).	41
Figure 3.3	The experimental setup of the test.	42
Figure 3.4	The 4830 Servopulser Control unit (SHIMADZU, 2018).	43
Figure 3.5	The range of the tested stroke and the testing position on MR damper (unit is in mm).	43
Figure 3.6	Graph of (a) force (kN) versus displacement (mm), and (b) force (kN) versus velocity (mm/s) plots at 0.4 Hz sinusoidal excitation.	44
Figure 3.7	Graph of (a) force (kN) versus displacement (mm), and (b) force (kN) versus velocity (mm/s) plots at 0.8 Hz sinusoidal excitation.	45
Figure 3.8	Graph of (a) force (kN) versus displacement (mm), and (b) force (kN) versus velocity (mm/s) plots at 1.2 Hz sinusoidal excitation.	46
Figure 3.9	Graph of (a) force (kN) versus displacement (mm), and (b) force (kN) versus velocity (mm/s) plots at 1.6 Hz sinusoidal excitation.	46
Figure 3.10	Graph of (a) force (kN) versus displacement (mm), and (b) force (kN) versus velocity (mm/s) plots at 2.0 Hz sinusoidal excitation.	47

Figure 3.11	Graph of (a) force (kN) versus current (A) versus displacement (mm), and (b) force (kN) versus current (A) versus velocity (mm/s) (in 3D) at constant 0.4 Hz sinusoidal excitation.	48
Figure 3.12	Graph of (a) force (kN) versus current (A) versus displacement (mm), and (b) force (kN) versus current (A) versus velocity (mm/s) (in 3D) at constant 0.8 Hz sinusoidal excitation.	48
Figure 3.13	Graph of (a) force (kN) versus current (A) versus displacement (mm), and (b) force (kN) versus current (A) versus velocity (mm/s) (in 3D) at constant 1.2 Hz sinusoidal excitation.	49
Figure 3.14	Graph of (a) force (kN) versus current (A) versus displacement (mm), and (b) force (kN) versus current (A) versus velocity (mm/s) (in 3D) at constant 1.6 Hz sinusoidal excitation.	50
Figure 3.15	Graph of (a) force (kN) versus current (A) versus displacement (mm), and (b) force (kN) versus current (A) versus velocity (mm/s) (in 3D) at constant 2.0 Hz sinusoidal excitation.	51
Figure 3.16	Forces versus current of RD-8040-1 damper (compression and tension direction).	51
Figure 3.17	The susceptibility of RD-8040-1 to the applied current (tension direction).	52
Figure 3.18	Graph of (a) force versus displacement and, (b) force versus velocity at constant 0 A input current.	53
Figure 3.19	Graph of (a) force versus displacement and, (b) force versus velocity at constant 0.5 A input current.	54
Figure 3.20	Graph of (a) force versus displacement and, (b) force versus velocity at constant 1 A input current.	55
Figure 3.21	Graph of (a) force versus frequency versus displacement, and (b) force versus frequency versus velocity (in 3D) at constant 0 A input current.	55
Figure 3.22	Graph of (a) force versus frequency versus displacement, and (b) force versus frequency versus velocity (in 3D) at constant 0.5 A input current.	56
Figure 3.23	Graph of (a) force versus frequency versus displacement, and (b) force versus frequency versus velocity (in 3D) at constant 1.0 A input current.	57
Figure 3.24	The Stribeck effect at excitation frequency of 2 Hz and applied current of 1 A.	58

Figure 3.25	Energy dissipated in the hysteresis loop in (a) Energy versus Current and (b) Energy versus Frequency plots.	59
Figure 3.26	The energy dissipation versus frequency and current plots of RD-8040-1.	59
Figure 4.1	The methodology of parametric model optimization.	64
Figure 4.2	The value of Modified Bouc-Wen parameters as function of current and frequency; (a) β , (b) γ , (c) A, (d) k_1 , (e) k_0 , (f) c_0 , (g) c_1 , and (h) f_0 .	67
Figure 4.3	Comparisons between the empirical data and simulation data at frequency of 0.4 Hz for (a) force versus displacement and, (b) force versus velocity.	70
Figure 4.4	Comparisons between the empirical data and simulation data at frequency of 0.8 Hz for (a) force versus displacement and, (b) force versus velocity.	71
Figure 4.5	Comparisons between the empirical data and simulation data at frequency of 1.2 Hz for (a) force versus displacement and, (b) force versus velocity.	72
Figure 4.6	Comparisons between the empirical data and simulation data at frequency of 1.6 Hz for (a) force versus displacement and, (b) force versus velocity.	73
Figure 4.7	Comparisons between the empirical data and simulation data at frequency of 2 Hz for (a) force versus displacement and, (b) force versus velocity.	74
Figure 5.1	The model of transtibial prosthetic limb with MR damper (Nordin et al., 2018).	78
Figure 5.2	Free body diagram of transtibial prosthetic limbs at heel strike.	78
Figure 5.3	The block diagram of transtibial prosthetic limb system.	81
Figure 5.4	The block diagram of transtibial prosthetic limb model.	81
Figure 5.5	The block diagram of damper controller or inverse Modified Bouc-Wen model where current estimation block diagram use <i>vpasolve</i> function (MATLAB function).	81
Figure 5.6	The block diagram of MR damper or Modified Bouc-Wen model where it consist of (a) overall block diagram of Modified Bouc-Wen model, (b) Equation 1 block diagram, (c) Equation 2 block diagram, and (d) Equation 3 block diagram.	83

Figure 5.7	Block diagram of disturbance rejection for prosthetic limb.	84
Figure 5.8	Comparison of body travel (m) performance between ground reaction force (<i>GRF</i>), Open-loop response, Controller response K_1 , Controller response K_2 and Controller response K_3 .	88
Figure 5.9	Comparison of body acceleration (m/s^2) performance between ground reaction force (<i>GRF</i>), Open-loop response, Controller response K_1 , Controller response K_2 and Controller response K_3 .	89
Figure 5.10	Comparison of body velocity (m/s) performance between ground reaction force (<i>GRF</i>), Open-loop response, Controller response K_1 , Controller response K_2 and Controller response K_3 .	89
Figure 5.11	Comparison of Control force (N) performance between ground reaction force (<i>GRF</i>), Open-loop response, Controller response K_1 , Controller response K_2 and Controller response K_3 .	90
Figure 5.12	Comparison of current estimation (A) performance between Acceleration Controller (Controller K_1), Balance Controller (Controller K_2) and Suspension Controller (Controller K_3).	91
Figure 5.13	Graph of suspension/body travel of an amputees at (a) 2.5 m/s walking speed of 80 kg body mass, (b) 4.5 m/s walking speed of 70 kg body mass, (c) 4.5 m/s walking speed of 80 kg body mass, and (d) 4.5 m/s walking speed of 90 kg body mass.	93
Figure 5.14	Graph of suspension/body acceleration of an amputees at (a) 2.5 m/s walking speed of 80 kg body mass, (b) 4.5 m/s walking speed of 70 kg body mass, (c) 4.5 m/s walking speed of 80 kg body mass, and (d) 4.5 m/s walking speed of 90 kg body mass.	96
Figure 5.15	Graph of suspension/body velocity of an amputees at (a) 2.5 m/s walking speed of 80 kg body mass, (b) 4.5 m/s walking speed of 70 kg body mass, (c) 4.5 m/s walking speed of 80 kg body mass, and (d) 4.5 m/s walking speed of 90 kg body mass.	98
Figure 5.16	Graph of suspension force of damper at (a) 2.5 m/s walking speed of 80 kg body mass, (b) 4.5 m/s walking speed of 70 kg body mass, (c) 4.5 m/s walking speed of 80 kg body mass, and (d) 4.5 m/s walking speed of 90 kg body mass.	100

LIST OF SYMBOLS

η_p	Plastic Viscosity
τ	Shear Stress
γ	Shear Strain
$\dot{\gamma}$	Shear Rate
τ_y	Yield Stress
H	Magnetic Field Strength (A/m)
M	Magnetization (A/m)
C	Curie Constant of Material (K)
T	Temperature (K)
f_c	Frictional Force
f_0	Offset Force
c_0, c_1	Damping Coefficient
F	Damping Force
k_0, k_1	Spring Stiffness
x_0	Initial Deflection
α	Scaling Factor
$z, A, \beta, \gamma, n, \delta$	Hysteretic Parameters
A_m	Amplitude
f	Frequency (Hz)
t	Time (s)
i	Current (A)
m_b	Mass of Body
s_w	Horizontal Walking Speed
W_g	Weight of Body
L_c	Walking Stride Length
t_c	Contact Time
t_a	Aerial Time
t_{step}	Time Step

LIST OF ABBREVIATIONS

SACH	Solid Ankle Cushioned Heel
ESAR	Energy Storage and Return
IP	Intelligent Prosthesis
MR	Magnetorheological fluid
UTM	Universal Testing Machine
GA	Genetic Algorithm
FLS	Fuzzy Logic System
ANN	Artificial Neural Network
IPGA	Intergeneration Projection Genetic Algorithm
NGSA II	Non-dominated Sorting Genetic Algorithm II
PSO	Particle Swarm Optimization
PID	Proportional-Integral-Derivative
LQG	Linear Quadratic Gaussian
LQR	Linear Quadratic Regulator
H_∞	H-infinity
FTM	Fatigue Testing Machine
LVDT	Linear Variable Differential Transformer
GRF	Ground Reaction Force

CHAPTER ONE

INTRODUCTION

1.1 BACKGROUND OF THE STUDY

Daily human activities are mostly required for humans to mobilize from a place to another. Walking and running are the methods of human locomotion, using two legs as support and propulsion to move around. However, for amputees, especially transtibial (below-knee) amputees require prosthesis to support them in walking and improving their gait.

A lot of research on designing and improving the performance of transtibial prosthetic limbs has done over a decade. The most common available transtibial prosthetic limbs are Solid Ankle Cushioned Heel (SACH) at which, the walking shock absorption comes from the cushioned heel. However, the ability of SACH to absorb the shock or damping forces is limited. Energy Storage and Return (ESAR) foot is another option, where it can absorb a significant amount of shock or damping forces during the loading phase and release it later during push-off (Grimmer et al., 2016). Nevertheless, both devices are passive, in which unable to provide mechanized energy or positive power to adjust the amputee's gait cycle and help them to propel forward (Lemoine, 2016).

Active transtibial prosthetic limbs contain powered element to support in locomotion for the whole gait cycle (Hitt, Sugar, Holgate, & Bellman, 2010). Power Knee by Össur, Intelligent Prosthesis (IP) by Blatchford, Intelligent Knee by Nabtesco and C-Leg by Otto Bock are the examples of available powered actuated prosthetic limbs (Grimmer et al., 2016). These devices are actuated using either DC motor, pneumatic, or hydraulic actuators. Power Knee, for example, provides maximum

support at knee joint for active bending (flexion) and extension during walking, helping amputees to go further. Apart from that, Grimmer et al. (2016) proposed an improved version of the active prosthetic ankle by Markowitz et al. (2011) to mimic the behaviour of human ankle movement. This device emphasizes dorsiflexion and plantarflexion control to adapt to terrain variation and walking speed. Even though active prosthesis can support amputees for the whole gait cycle and provide positive power e.g., climbing stairs, more energy is required since they are continuously active (Lui, Awad, Abouhossein, Dehghani-Sanij, & Messenger, 2015). Figure 1.1 shows the example of available passive and active transtibial prosthetic limbs.



Figure 1.1 Passive transtibial prosthetic limbs (ESAR) (left side) and active transtibial prosthetic limbs (right side) (retrieved from “Feet and Ankles”, 2018).

Before design the transtibial prosthetic limbs, the basic gait cycle is discussed. It is owing to understand the gait cycle help to better detect the critical phase that acquired much more attention in designing the prosthesis. Gait is known as a manner of walking, and the gait cycle defined as the period of repetitive events of walking. The single gait cycle is measured where one foot contacts the ground until the same foot touches the ground again in locomotion. The gait cycle is divided into two main phases: the stance phase and the swing phase, as shown in Figure 1.2. Generally, the stance phase occupies approximately 60% of the single gait cycle and 40% by swing phase.

However, this varies with walking speed, where the swing phase will be more prolonged, and the stance phase will be shorter when the rate increased (Whittle, 2007).

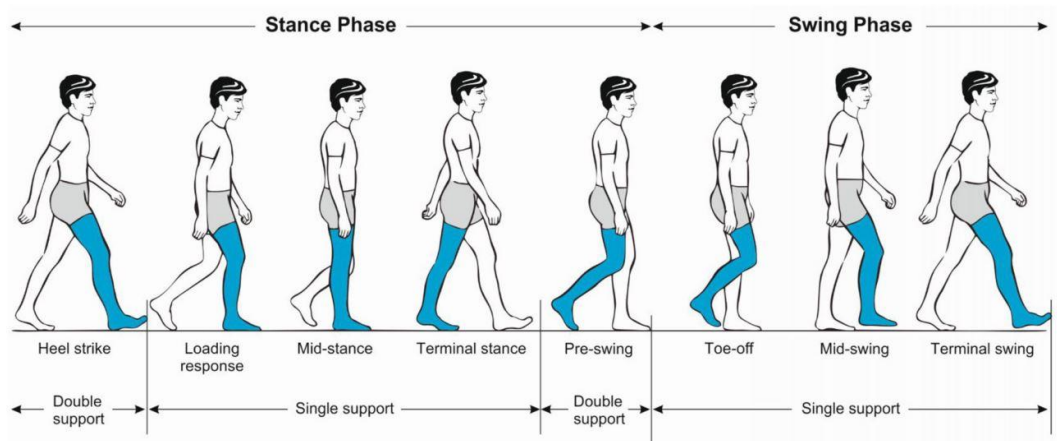


Figure 1.2 Positions of legs during single gait cycle (blue) (Pirker & Katzenschlager, 2016).

A detail of the gait cycle for stance phase recognizes five significant events which are:

- 1) Heel strike
- 2) Loading response,
- 3) Mid-stance,
- 4) Terminal stance, and
- 5) Pre-swing.

While the swing phase divided into three significant events which are:

- 1) Toe-off or initial swing,
- 2) Mid-swing, and
- 3) Terminal swing (J. Park, Yoon, Kang, & Choi, 2016).

At the beginning of a stance phase, a transient force known as a heel strike is generated. The heel strike transient represents an exchange of momentum when the foot contacts the ground, terminating the previous movement (Addison & Lieberman, 2015;

Tongen & Wunderlich, 2012; Zinner & Sperlich, 2016). Figure 1.3 shows the ground reaction force in the vertical direction from a walk experimented by Whittle (2007). The heel strike transient happens typically at 10 ms to 20 ms and is seen as a short spike of force.

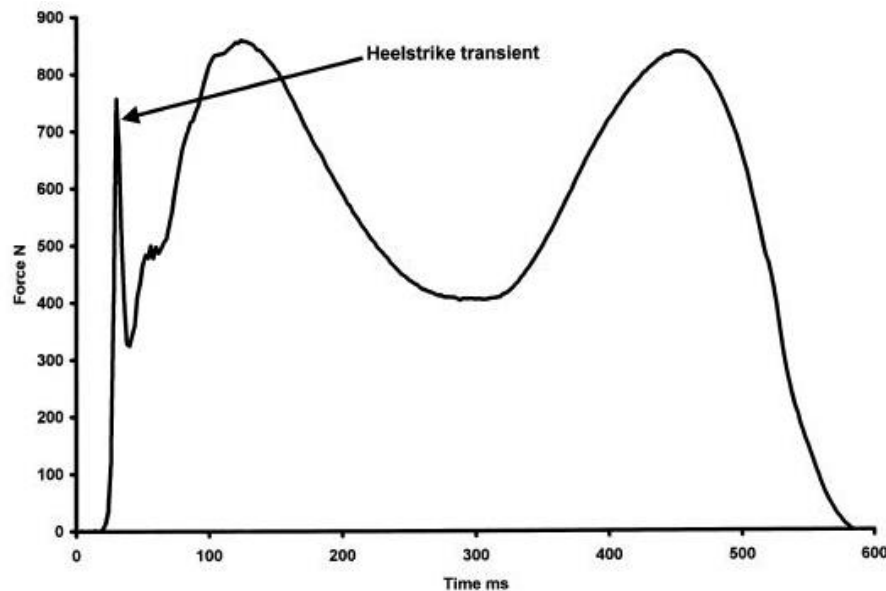


Figure 1.3 Plot of vertical ground reaction force (N) against time (ms) (Whittle, 2007).

It has been found that the resulting shock wave from the heel strike may produce damage to the human body. The previous researchers suggested there are possible shock-related injuries due to the heel strike transient, including headaches and osteoarthritis (degenerative joint disease) (Light, McLellan, & Klenerman, 1980), stress fractures (Dickinson, Cook, & Leinhardt, 1985), plantar fasciitis (D. Singh, Angel, Bentley, & Trevino, 1997), chronic low back pain, degeneration of cartilage (C. Y. Lin, Chuang, & Cortes, 2017) and prosthetic joint loosening (Whittle, 2007).

Possible solutions to reduce the effect of heel strike transient, especially prosthetic limb users, is the use of a heel pad (Jorgensen & Ekstrand, 1988). This is the earliest solution to encounter the heel strike, yet it only able to absorb the transient force approximately up to 47 to 66% (Whittle, 2007). The control of plantar flexion of ankle

and knee is another possible solution where it presumes to provide shock absorption immediately after initial contact (Ebbeling, Hamill, & Crussemeyer, 1994). However, plantar flexion of ankle and knee occupies at 80 ms and 150 ms respectively slower than heel strike transient (20 ms), thus impossible to protect the leg from the transient force (Whittle, 2007).

Hence, to provide a better solution for the need for shock absorption for transtibial amputees, a device that is damper-based shock absorber is suggested. A semi-active damper is adopted in the design of the prosthetic limb to capture the advantages of passive damper, along with performing as good as an active damper. The design also will mainly focus on reducing the heel strike transient effect. This research describes the use of a Magnetorheological damper or MR damper (semi-active damper) in the transtibial prosthetic limb. The work is initiated with understanding the parameters that affect the performance of MR damper. A controller is then designed so that the system is capable of reducing vibrations at various walking speeds.

1.2 PROBLEM STATEMENT

When human in motions either walking or running, human lower limb's damping characteristic changes to provide proper movement condition. However, uncontrolled exposure to vibration especially during heel strike may lead to injuries or prosthesis malfunction. Having an adaptive capability in artificial prosthesis for lower limb amputees is necessary to provide essential movements and attenuate unwanted vibration. To design an adaptive prosthetic limbs, a semi-active damping device which is Magnetorheological Fluid (MR) damper is proposed. This device have the capabilities to attenuate broadband vibration without consuming much power consumption.

However, major drawbacks that restrict the applications of MR damper are nonlinear hysteresis force-velocity and force-displacement characteristic. Thus, to design high efficiencies of MR damper applications, an accurate mathematical model that can take full advantages of this device is required. Developing and utilizing these devices become more challenging due to inherent nonlinear nature of the dampers. In this study, the dynamic response of the MR damper is investigated by testing the damper under different conditions. Then, the dynamic models of the damper is developed using a proposed method. The proposed method will help for further research as reference on how to estimate the dynamic models. For further investigation, the proposed dynamic models are expected to be applied on practical applications, prosthetic limb for example. On these bases, semi-active controller system, consist of a system controller and a damper controller are required. System controller is to generate desired force based on dynamic response of a plant while the damper controller is to track the generated damping force by adjusting the value of voltage or current. The inverse dynamic model of the damper is required to design the damper controller. The detail of the design will be explained in the next chapter.

1.3 RESEARCH OBJECTIVES

The objectives of this research are:

1. To understand the behavior of MR damper under various input current and damping frequency.
2. To estimate and optimize the parameters of the MR damper models based on experimental result.
3. To control the MR damper for transtibial prosthetic limb application.

1.4 RESEARCH METHODOLOGY

The methodology to achieve the research objectives is adopted as follows (flow chart of research methodology may refer to Figure 1.4):

- a) Exploring the MR damper background and analyzing its problems through an extensive literature review

Carry out an extensive study of the published works to fully comprehend and value the significance, scope, and underpinnings of this research. The outcome of this study should be the identification of critical parameters or factors to improve the dynamic range of MR damper.

- b) Experimental investigation

Carry out an experimental study to test the MR damper's dynamic behavior under the variation of parameters. The force-displacement and force-velocity relationship are the expected outcome of the test.

- c) Parametric optimization of MR damper model

Identify the available MR damper model and perform parametric optimization on the model by comparing with the experimental result. The outcome of the task is to have a mathematical model in which able to describe the actual performance of MR damper.

- d) Controller design

Design controller to control MR damper for prosthetic limb application. The expected outcome from the task is to have a robust control algorithm to control the prosthetic limb and a controller (inverse MR damper model) to control the MR damper.